ORIGINAL ARTICLE

# Three-dimensional prediction of nose morphology in Chinese young adults: a pilot study combining cone-beam computed tomography and 3dMD photogrammetry system

Guang Chu[1,2] · Jia-min Zhao[1,2] · Meng-qi Han[1,2] · Qing-nan Mou[1,2] · Ling-ling Ji[1,2] · Hong Zhou[1,2] · Teng Chen[3] · Shao-yi Du[4] · Yu-cheng Guo[1,2,4]

## Abstract

The nose is the most prominent part of the face and is a crucial factor for facial esthetics as well as facial reconstruction. Although some studies have explored the features of external nose and predicted the relationships between skeletal structures and soft tissues in the nasal region, the reliability and applicability of methods used in previous studies have not been reproduced. In addition, the majority of previous studies have focused on the sagittal direction, whereas the thickness of the soft tissues was rarely analyzed in three dimensions. A few studies have explained the specific characteristics of the nose of Chinese individuals. The aim of this study was to investigate the relationship between the hard nasal structures and soft external nose in three dimensions and to predict the morphology of the nose based on hard-tissue measurements. To eliminate the influence of low resolution of CBCT and increase the accuracy of measurement, three-dimensional (3D) images captured by cone-beam computed tomography (CBCT) and 3dMD photogrammetry system were used in this study. Twenty-six measurements (15 measurements for hard tissue and 11 measurements for soft tissue) based on 5 craniometric and 5 capulometric landmarks of the nose of 120 males and 120 females were obtained. All of the subjects were randomly divided into an experimental group (180 subjects consisting of 90 males and 90 females) and a test group (60 subjects consisting of 30 males and 30 females). Correlation coefficients between hard- and soft-tissue measurements were analyzed, and regression equations were obtained based on the experimental group and served as predictors to estimate nasal morphology in the test group. Most hard- and soft-tissue measurements appeared significantly different between genders. The strongest correlation was found between basis nasi protrusion and nasospinale protrusion (0.499) in males, and nasal height and nTr-nsTr (0.593) in females. For the regression equations, the highest value of $R^2$ was observed in the nasal bridge length in males (0.257) and nasal tip protrusion in females (0.389). The proportion of subjects with predicted errors < 10% was over 86.7% in males and 70.0% in females. Our study proved that a combined CBCT and 3dMD photogrammetry system is a reliable method for nasal morphology estimation. Further research should investigate other influencing factors such as age, skeletal types, facial proportions, or population variance in nasal morphology estimation.

**Keywords** Craniofacial reconstruction · Nasal region · CBCT · 3dMD · Nose morphology · Three-dimensional

✉ Shao-yi Du
dushaoyi@xjtu.edu.cn

✉ Yu-cheng Guo
xjtu-guoyucheng@163.com

[1] Key Laboratory of Shaanxi Province for Craniofacial Precision Medicine Research, College of Stomatology, Xi'an Jiaotong University, 98 XiWu Road, Xi'an 710004, Shaanxi, People's Republic of China

[2] Department of Orthodontics, Stomatological Hospital of Xi'an Jiaotong University, 98 XiWu Road, Xi'an 710004, Shaanxi, People's Republic of China

[3] College of Medicine and Forensics, Xi'an Jiaotong University Health Science Center, 76 West Yanta Road, Xi'an 710004, Shaanxi, People's Republic of China

[4] Institute of Artificial Intelligence and Robotics, College of Artificial Intelligence, Xi'an Jiaotong University, 28 Xianning West Road, Xi'an 710049, Shaanxi, People's Republic of China

# Introduction

Craniofacial reconstruction is the technique that uses skeleton information acquired from unknown human skull to predict the morphology of soft tissues [1] and plays a significant role in forensic practice. To achieve a reliable and accurate depiction of the face, basic knowledge of the relationship between craniofacial skeletal and facial soft tissue is crucial because it will directly influence the accuracy of individual facial reconstruction [2]. Numerous studies have analyzed the interrelationship between the hard and soft tissues of the face, especially facial soft-tissue thickness [3–6]. The nose serves as a special facial feature in the recognition of individuals and is closely associated with other facial structures [7]. Therefore, the importance of nose reconstruction should not be neglected.

The profile of the nose, as the prominent part of the midface, is vital in facial recognition and is of great importance in forensic facial reconstruction [2, 8]. In traditional nose reconstruction techniques, the nasal bone, piriform aperture, anterior nasal spine (ANS), and other skeleton landmark points were applied to predict an individual's nose morphology [8–12]. In addition, as the underlying bone of the nose only comprises a minor proportion of the mid-facial cranium, the three-dimensional distances between skeletal and soft-tissue landmark planes are also considered as predictors of nose morphology [13, 14]. However, traditional researches that depicted the connections between skull and external nose were mostly based on skeletal or cadaveric samples [15, 16], which had obvious limitations: the inevitable shrinkage and distortion of soft tissues caused by dehydration after death, resulting in measurement errors [17].

With the development of radiology and imageology, aside from puncture [18, 19], many different new techniques have been applied to assess nose morphology in living populations, including ultrasonography (US) [20–22], cephalometric radiographic imaging (CXI) [23, 24], computed tomography (CT) [8, 13, 25, 26], and magnetic resonance imaging (MRI) [27]. Among all of these techniques, CT may be the most widely used due to its low cost and high spatial resolution on both hard and soft tissues. However, traditional CT scans have two limitations. One is the supination effect on the head due to the horizontal position of the patient during scanning and thus CT images cannot be captured at physiological status [14, 28, 29]. The other is that the slice thickness of scanning ranges from 0.6 to 1.5 mm, which might increase errors in measurement. Recently, cone-beam computed tomography (CBCT) scanning, a technique that allows patients to maintain a natural position for head during scanning with a cone-shaped X-ray beam, has been widely used in facial examination [13, 14]. Lower cost, reduced radiation dose, and higher spatial resolution have also made it possible to replace CT scanning in nose reconstruction [14].

Nevertheless, CBCT has its own drawbacks. For example, to maintain the natural position of the head, a fixed device is needed to support the chin, which would induce compression and distortion of facial muscular. In addition, the facial soft tissue scanned by CBCT only reveals the contour of the face, the minor features and specific details are mostly neglected, and thus, it is difficult to accurately analyze soft tissues in three dimensions. Recently, the appearance of three-dimensional (3D) photogrammetry technology has overcome these limitations. From an anthropometric perspective, non-contact 3dMD photogrammetry system has many advantages compared to other systems: precise reconstruction of the 3D face with high-resolution color, quantification of angles, linear distance, surface areas and volumes, establishment of 3D coordinate system for each landmark, and 3D surface images can be captured within 2 milliseconds [30, 31]. Although the use of digital 3D photogrammetry system has increased in oral and maxillofacial surgeries, studies on facial reconstruction in the forensic field are limited.

Several studies have employed CBCT scanning to analyze the relationship between the skeletal nasal bone and external nose morphology in different populations [13, 14]. These investigations have predicted the morphology of the face by angles or linear distances acquired from corresponding landmarks in different planes. However, the specific and detailed characteristics of the external nose in three dimensions have not been extensively investigated. Therefore, the aim of this study was to investigate the correlation between skeletal nasal bone and nose morphology based on CBCT and 3dMD photogrammetry system in three dimensions.

The objectives of this study were as follows:

(1) To investigate the sexual dimorphism in nasal dimensions of Chinese young adults;
(2) To establish specific regression equations to predict external nose morphology from nasal skeletal landmarks and evaluate the accuracy of the formulas in Chinese young adults; and
(3) To verify the accuracy of the measurement method for the nasal region by combining the CBCT and 3dMD techniques.

# Materials and methods

CBCT scans and 3dMD photogrammetry images of 240 young orthodontic patients (120 males and 120 females) aged between 20 and 30 years old were selected from the Department of Oral Radiology, the Stomatological Hospital of Xi'an Jiaotong University, Xi'an, Shaanxi, China. All of the scans and images were necessary for treatment planning and taken between March 2018 and February 2019. The

**Fig. 1** Five soft-tissue landmark points for matching the CBCT scans and 3dMD images
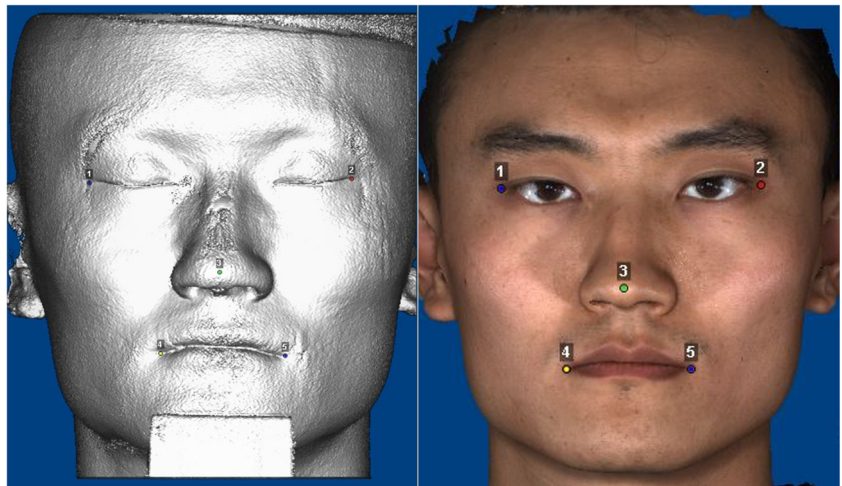
chronological age was calculated by subtracting the date of birth from the date of X-ray exposure. Subjects were excluded if they presented with any condition or disease might affect the morphology of the face (e.g., previous orthodontic treatment or orthognathic surgery history, long-term unilateral masticatory habit, obvious skeletal or external facial asymmetry, severe skeletal malocclusion or absence of upper anterior teeth). Only subjects with medium body mass index range (18.5–23.5) were included in the study.

All 240 subjects (120 males and 120 females) were randomly divided into an experimental group (90 males and 90 females) and test group (30 males and 30 females). The experimental group was used for developing regression equations, and the test group was used to verify the accuracy of these equations.



**Fig. 2** The integrated 3D digital image

## CBCT scans, 3dMD images, and superimposed 3D image reconstruction

CBCT scans were obtained using a CBCT scanner (KaVo 3D eXam i, Germany) with the following properties: 230 V, 5A, 50/60 Hz, and 1150VA. The CBCT scans were conducted with the use of reference ear plug (REP) and head posture aligner (HPA) to maintain a natural head position [32]. A 3D soft-tissue facial scan of each patient was captured by a 3dMD photogrammetry camera (3dMD, Atlanta, GA, USA), with a natural head position, relaxed facial expression, and with eyes looking straight ahead [33, 34].

The data on CBCT were saved in the DICOM format, whereas that of 3dMD was saved in the BMP format. Both formats were transformed into an image-processing software called Dolphin (version 11.8; Dolphin Imaging and Management Solutions, Chatsworth, CA, USA) and then integrated into a complete 3D digital image before measuring. To ensure the highest degree of superimposition in nasal region, five landmark points (left and right outer canthus, tip of nose, and left and right angulus oris) in the soft face were selected to match the CBCT scans and 3dMD images manually (Fig. 1). After integrating the CBCT scans and 3dMD images, the soft-tissue data from CBCT was removed and replaced by a 3dMD face mask. Therefore, the remaining skeletal skull (CBCT scans) and soft facial mask (3dMD images) were presented as the final 3D images for measurement (Fig. 2).

## Landmarks, planes, and measurements

Five craniometric landmarks [nasion (n), rhinion (rhi), nasospinale (ns), alare (al), and prosthion (pro)] were identified on the nasal bone and periphery of the nasal aperture (Fig. 3). As the corresponding external soft tissue, five capulometric landmarks [soft Nasion (N), Pronasale (Prn),

**Fig. 3** **a**, **b** Craniometric landmarks [nasion (n), rhinion (rhi), nasospinale (ns), alare (al) and prosthion (pro)] and planes on the nasal bone and periphery of the nasal aperture
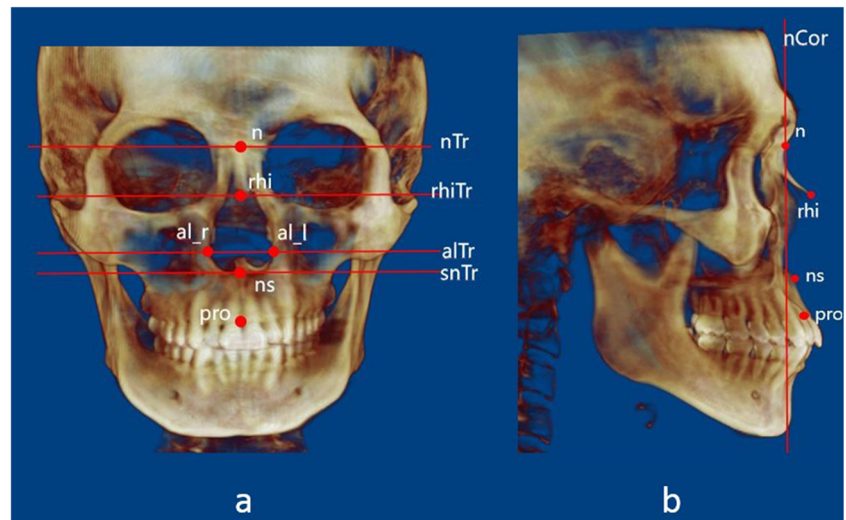


Subnasale (Sn), Ala (Al), and Labial superius (Ls)] were determined to represent the morphology of external nose (Fig. 4). Therefore, the three-dimensional angles and linear distance between landmarks can be presented to assess nasal morphology. Moreover, coronal, sagittal, and transverse planes were also considered to help depict the morphology of nose. The planes for the hard tissue included the nasion transverse plane (nTr), rhinion transverse plane (rhiTr), alare transverse plane (alTr), nasospinale transverse plane (nsTr), and nasion coronal plane (nCor). For soft tissues, we just used soft Nasion coronal plane (NCor), and pronasale coronal plane (PrnCor) to depict the protrusion of the nose. The definitions and abbreviations of the five craniometric and five capulometric landmarks are listed in Table 1. Figures 5 and 6 illustrate all of the measurements of the hard and soft tissues.

The hard-tissue measurements of the nose included three dimensions: nasal width, nasal height, nasal bone length, alare angle, nasal dorsum angle, nasal tip angle, nasolabial angle, rhinion protrusion, nasospinale protrusion, nTr-rhiTr, rhiTr-

alTr, alTr-nsTr, nTr-alTr, rhiTr-nsTr, and nTr-nsTr. To assess the soft-tissue morphology of the nose, Nasal bridge length, Nasal height, Nasal columella length, Alar width, Basis nasi angle, Alare angle, Nasal dorsum angle, Nasal tip angle, Nasolabial angle, Nasal tip protrusion, and Basis nasi protrusion were taken into consideration. A total of 26 measurements (15 for hard tissues and 11 for soft tissues) are demonstrated in Table 2. To discriminate the measurements between hard and soft tissue, we capitalized the initial letter of landmarks to represent the measurements of the soft tissues.

### Statistical analysis

To assess the reproducibility of the measurements, the integrated images of 20 subjects (experimental group consisting of 10 males and 10 females) were randomly selected to test inter- and intra-observer errors. The method error (ME) of the double registration for all measurements was calculated using Dahlberg's [35] formula:
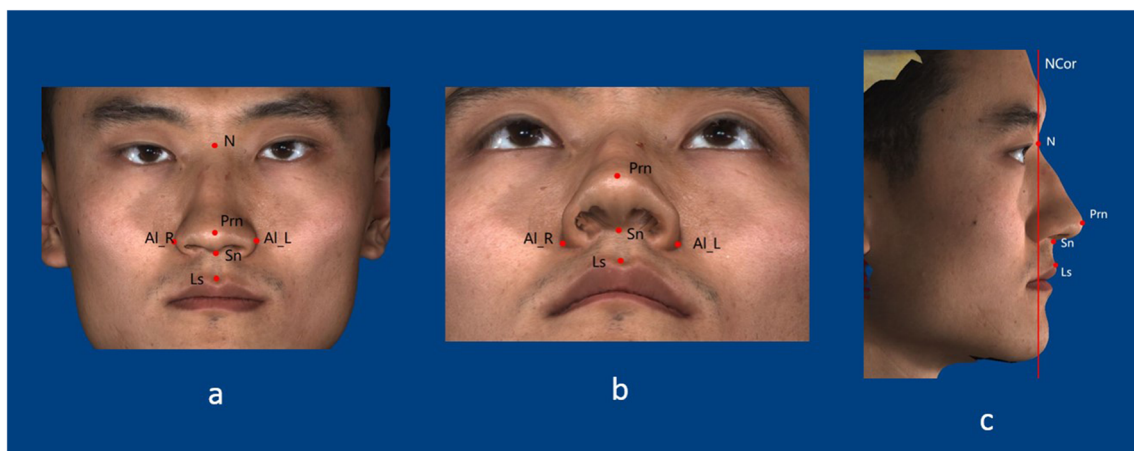


**Fig. 4** **a–c** Capulometric landmarks [soft Nasion (N), Pronasale (Prn), Subnasale (Sn), Ala (Al), and Labial superius (Ls)] and plane on external nose

**Table 1** Definition and abbreviation of craniometric and capulometric landmarks

| | Landmarks | Abbreviation | Definition |
|---|---|---|---|
| Craniometric | nasion | n | Mid sagittal point of suture between frontal bone and nasal bone |
| | rhinion | rhi | Most inferior end of suture between left and right nasal bone |
| | nasospinale | ns | Anterior tip of bony process of maxilla at the lower margin of anterior nasal opening |
| | alare | al | the most lateral point on the nasal aperture in the transverse plane |
| | prosthion | pro | Lowest point of the alveolar bone between the left and right upper first incisors |
| Capulometric | Soft nasion | N | the midpoint on the soft-tissue contour of the base of the nasal root at the level of the frontonasal suture |
| | Pronasale | Prn | Most protruded point of soft tissue nose |
| | Subnasale | Sn | Midpoint of the angle at the columella base where the lower border of nasal septum |
| | Ala | Al | Most lateral point on alar contour |
| | Labial superius | Ls | Midpoint of the vermilion line of the upper lip |

$$ME = \sqrt{\sum_{i=1}^{n} \frac{d_i^2}{2n}},$$

where $d$ is the difference between two measurements, and $n$ is the number of subjects. The error will be considered acceptable in the study if the deviation is < 2 mm [14]. Additionally, intra-class correlation coefficient (ICC) was also used to evaluate inter- and intra-rater agreement of all measurements.

Means and standard deviations of measurements were calculated for each group. An independent $t$ test was used to test gender differences of measurements, and significance was set as $P < 0.05$. Pearson correlation analysis among measurements was used to explore the interrelationship between hard nasal bone and external soft tissue of nose. Stepwise multiple regression analysis was used to develop specific formulas to predict the soft-tissue morphology based on measurements of the hard tissues. All of the statistical analyses were conducted with Statistical Product and Service Solutions (SPSS) software, version 18.0 for Windows.

## Results

The result of Dahlberg's test proved that all landmarks were reproducible (0.51–1.63 mm). For the coincidence tests, the results of ICC in 26 measurements ranged from 0.893 to 0.948 and from 0.793 to 0.877 for the intra- and inter-rater agreement, respectively, which indicated a high degree of intra- and inter- observer agreement. The mean age of the 240 subjects was $25.15 \pm 5.18$ years. For the experimental group, the mean ages were $24.61 \pm 5.56$ and $25.66 \pm 4.97$ years for males and females, respectively. For the test group, the mean age was $25.71 \pm 4.83$ years for males and $24.68 \pm 5.20$ years for females. There were no significant age difference found between males and females in the two groups.

The means and standard deviations of the measurements involving hard nasal bone for males and females are shown in Table 3. Most of the hard-tissue measurements (nasal width, nasal height, nasal bone length, alare angle, nasal tip angle, rhinion protrusion, nTr-rhiTr, rhiTr-alTr, nTr-alTr, rhiTr-nsTr, and nTr-nsTr) were significantly different between males and females, except for the nasal dorsum angle, nasolabial angle, nasospinale protrusion, and alTr- nsTr. In all of the measurements with significant differences, the males showed higher values compared to the females, except for the alare angle and nasal tip angle. However, the soft-tissue measurement values shown in Table 4 indicate that Nasal bridge length, Nasal height, Nasal columella length, Alar width, Alare angle, and Nasal tip protrusion were significantly different between males and females. However, in terms of Basis nasi angle, Nasal dorsum angle, Nasal tip angle, Nasolabial angle, and Basis nasi protrusion, no significant differences were observed between the sexes. In terms of soft tissues, the males showed higher values compared to the females.

Correlation coefficients are established in Tables 5 and 6 to explore the interrelationship between external nose morphology and hard nasal bone in males and females. Overall, the correlation coefficients ranged from 0.228 to 0.499 and from 0.247 to 0.593 in males and females, respectively. According to the results, there were at least one to eight craniometric measurements showing significant correlations with each capulometric measurement. For males, Nasal bridge length showed a strong correlation with five hard-tissue measurements (nasal height 0.354, nasal bone length 0.375, alTr-nsTr 0.305, nTr-alTr 0.277, and nTr-nsTr 0.399), and the strongest correlation was found between Basis nasi protrusion and nasospinale protrusion (correlation coefficient 0.499). For females, Nasal height showed a strong correlation with eight hard-tissue measurements (nasal height 0.402, nasal bone length 0.585, nasal dorsum angle 0.278, rhinion protrusion 0.316, nTr-rhiTr 0.416, alTr-nsTr 0.256, nTr-alTr 0.500, and nTr-nsTr 0.593), whereas the strongest correlation was
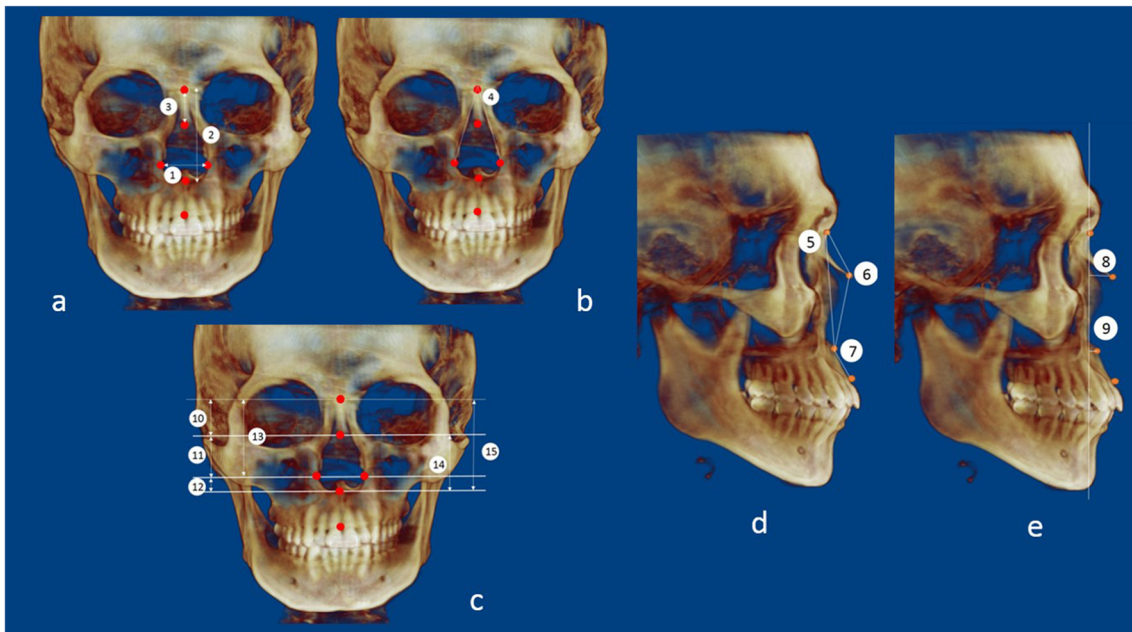
**Fig. 5** **a–e** Craniometric measurements on hard tissues (1. nasal width; 2. nasal height; 3. nasal bone length; 4. alare angle; 5. nasal dorsum angle; 6. nasal tip angle; 7. nasolabial angle; 8. rhinion protrusion; 9. nasospinale protrusion; 10. nTr-rhiTr; 11. rhiTr-alTr; 12. alTr-nsTr; 13. nTr-alTr; 14. rhiTr-nsTr; and 15. nTr-nsTr)

observed between Nasal height and nTr-nsTr (correlation coefficient 0.593). However, according to our study, there were several measurements, including Nasolabial angle in males and Nasal dorsum angle in females that showed no significant coefficients between hard tissue and corresponding soft-tissue measurements.

All of the significant correlation measurements were used in establishing stepwise multiple regression equations for predicting the morphology of the external nose in males and females (Tables 7 and 8). The $R^2$ of all the established formulas ranged from 0.038 to 0.257 in males and 0.014 to 0.389 in females. In males, the highest value of $R^2$ (0.257) appeared in



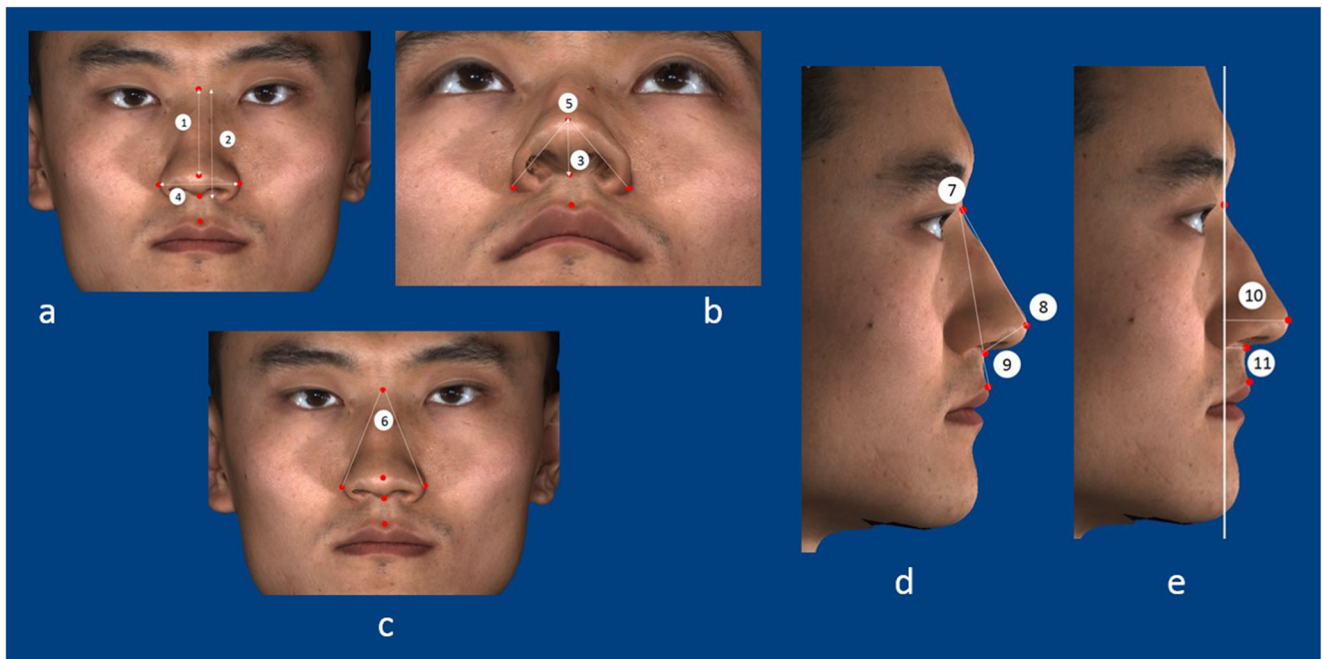**Fig. 6** **a–e** Capulometric measurements on soft tissues (1. Nasal bridge length; 2. Nasal height; 3. Nasal columella length; 4. Alar width; 5. Basis nasi angle; 6. Alare angle; 7. Nasal dorsum angle; 8. Nasal tip angle; 9. Nasolabial angle; 10. Nasal tip protrusion; and 11. Basis nasi)

**Table 2**　The definition of each measurement in hard-tissue nasal bone and external nose

|  | Measurement | Meaning or explanation |
|---|---|---|
| Hard tissue | nasal width | Linear distance between left and right alare (al) points |
|  | nasal height | Linear distance between nasion (n) and right nasospinale (ns) points |
|  | nasal bone length | Linear distance between nasion (n) and right rhinion (rhi) points |
|  | alare angle | Angulation calculated from intersecting lines drawn from the left alare (al) to nasion (n) points and from right alare (al) to nasion (n) points (al–n–al) |
|  | nasal dorsum angle | Angulation calculated from intersecting lines drawn from the left nasospinale (ns) to nasion (n) points and from rhinion (rhi) to nasion (n) points (ns–n–rhi) |
|  | nasal tip angle | Angulation calculated from intersecting lines drawn from the nasion (n) to rhinion (rhi) points and from nasospinale (ns) to rhinion (rhi) points (n–rhi–ns) |
|  | nasolabial angle | Angulation calculated from intersecting lines drawn from the rhinion (rhi) to nasospinale (ns) points and from prosthion (pro) to nasospinale (ns) points (rhi–ns–pro) |
|  | rhinion protrusion | Linear distance between rhinion (rhi) point and nasion coronal plane (nCor) |
|  | nasospinale protrusion | Linear distance between nasospinale (ns) point and nasion coronal plane (nCor) |
|  | nTr-rhiTr | Linear distance between nasion transverse plane (nTr) and rhinion transverse plane (rhiTr) |
|  | rhiTr-alTr | Linear distance between rhinion transverse plane (rhiTr) and alare transverse plane (alTr) |
|  | alTr-nsTr | Linear distance between alare transverse plane (alTr) and nasospinale transverse plane (nsTr) |
|  | nTr-alTr | Linear distance between nasion transverse plane (nTr) and alare transverse plane (alTr) |
|  | rhiTr-nsTr | Linear distance between rhinion transverse plane (rhiTr) and nasospinale transverse plane (nsTr) |
|  | nTr-nsTr | Linear distance between nasion transverse plane (nTr) and nasospinale transverse plane (nsTr) |
| Soft tissue | Nasal bridge length | Linear distance between the Nasion (N) and Pronasale (Prn) points |
|  | Nasal height | Linear distance between the Nasion (N) and Subnasale (Sn) points |
|  | Nasal columella length | Linear distance between the Subnasale (Sn) and Pronasale (Prn) points |
|  | Alar width | Linear distance between the left and right Ala (Al) points |
|  | Basis nasi angle | Angulation calculated from intersecting lines drawn from the left Ala (Al) to Pronasale (Prn) points and from right Ala (Al) to Pronasale (Prn) points (Al–Prn–Al) |
|  | Alare angle | Angulation calculated from intersecting lines drawn from the left Ala (Al) to Nasion (N) points and from right Ala (Al) to Nasion (N) points (Al–N–Al) |
|  | Nasal dorsum angle | Angulation calculated from intersecting lines drawn from the Subnasale (Sn) to Nasion (N) points and from Pronasale (Prn) to Nasion (N) points (Sn–N–Prn) |
|  | Nasal tip angle | Angulation calculated from intersecting lines drawn from the Nasion (N) to Pronasale (Prn) points and from Subnasale (Sn) to Pronasale (Prn) points (N–Prn–Sn) |
|  | Nasolabial angle | Angulation calculated from intersecting lines drawn from the Pronasale (Prn) to Subnasale (Sn) points and from Labial superius (Ls) to Subnasale (Sn) points (Prn–Sn–Ls) |
|  | Nasal tip protrusion | Linear distance between Pronasale (Prn) point and Nasion coronal plane (NCor) |
|  | Basis nasi protrusion | Linear distance between Subnasale (Sn) point and Nasion coronal plane (NCor) |

Nasal bridge length: 0.215 × nasal bone length + 0.096 × nasal height + 0.459 × (alTr - nsTr) + 0.117 × (nTr-nsTr) + 31.101. However, the lowest value of $R^2$ (0.038) was observed in Nasal dorsum angle: − 0.028 × nasal tip angle + 19.936. In females, the formulas with the highest and lowest $R^2$ values were observed in Nasal tip protrusion: 0.309 × nasal height + 0.027 × rhinion protrusion + 0.358 × nasospinale protrusion + 0.182 × (rhiTr -alTr) + 0.037 × (nTr - alTr) + 0.118 × (nTr - nsTr) - 6.322 ($R^2$ = 0.389) and Nasal columella length: − 0.033 × (nTr - alTr) + 0.176 × (nTr - nsTr) + 8.923 ($R^2$ = 0.014), respectively.

Finally, the established specific stepwise multiple regression equations for prediction of soft-tissue measurements based on corresponding hard-tissue values were used to verify the accuracy in test group. The mean of (MV-PV), mean of |MV-PV|, maximum of |MV-PV|, minimum of |MV-PV|, proportion of subjects with errors within 3 mm or 5°, and proportion of subjects with errors < 10% were calculated (Tables 9 and 10). In males, the mean of |MV-PV| for length measurements ranged from 1.23 ± 0.88 mm to 3.14 ± 2.39 mm and from 1.29 ± 0.64° to 5.17 ± 3.65° for angle measurements. Taking the maximum of |MV-PV| in consideration, the value

**Table 3** Means and standard deviations of the measurements for hard tissues (mm) in Chinese young adults

| Measurements | Total (n = 180) | | Male (n = 90) | | Female (n = 90) | | Sex difference |
| --- | --- | --- | --- | --- | --- | --- | --- |
| | Mean | SD | Mean | SD | Mean | SD | p value |
| nasal width | 23.65 | 2.09 | 24.12 | 2.26 | 23.19 | 1.79 | 0.003* |
| nasal height | 24.31 | 3.36 | 25.47 | 3.00 | 23.15 | 3.31 | 0.000* |
| nasal bone length | 52.22 | 3.98 | 54.55 | 3.73 | 49.90 | 2.65 | 0.000* |
| alare angle | 28.10 | 2.85 | 27.38 | 2.87 | 28.82 | 2.65 | 0.001* |
| nasal dorsum angle | 22.00 | 10.02 | 22.37 | 4.28 | 21.64 | 13.54 | 0.626 |
| nasal tip angle | 141.54 | 12.14 | 138.98 | 15.38 | 144.11 | 6.83 | 0.004* |
| nasolabial angle | 155.31 | 13.61 | 153.93 | 17.25 | 156.7 | 8.43 | 0.172 |
| rhinion protrusion | 11.57 | 2.56 | 12.32 | 2.52 | 10.82 | 2.39 | 0.000* |
| nasospinale protrusion | 6.38 | 3.28 | 6.33 | 3.63 | 6.44 | 2.91 | 0.814 |
| nTr-rhiTr | 21.81 | 3.35 | 22.6 | 3.10 | 21.03 | 3.42 | 0.002* |
| rhiTr-alTr | 24.93 | 3.14 | 26.46 | 3.17 | 23.41 | 2.24 | 0.000* |
| alTr-nsTr | 5.45 | 1.52 | 5.43 | 1.55 | 5.46 | 1.50 | 0.876 |
| nTr-alTr | 46.75 | 3.99 | 49.07 | 3.45 | 44.44 | 3.07 | 0.000* |
| rhiTr-nsTr | 30.38 | 3.25 | 31.89 | 3.29 | 28.88 | 2.42 | 0.000* |
| nTr-nsTr | 52.20 | 4.114 | 54.5 | 3.59 | 49.91 | 3.24 | 0.000* |

ranged from 3.00 to 10.36 mm for length measurements and from 2.58° to 13.02° for angle measurements. The proportion of values with length or angle measurements errors within 3 mm or 5° were between 56.7 and 100%, and the proportion of measurements errors < 10% were between 83.3 and 100%. In females, the mean of |MV-PV| ranged from $1.15 \pm 0.94$ mm to $2.51 \pm 1.65$ mm and from $2.48 \pm 2.10°$ to $8.38 \pm 7.05°$ for the length and angle measurements, respectively. The maximum of |MV-PV| ranged from 3.62 to 7.22 mm for length measurements and from 7.94 to 23.29° for angle measurements. 50.0–93.3% of subjects with measurements errors within 3 mm or 5°and 70.0 to 100% subjects with errors < 10%. Moreover, no significant difference between the measured value and predicted value was observed in each measurement for both sexes according to the paired $t$ test.

## Discussion

The nose is the central feature of face that played a crucial role on facial esthetics. The position, size, shape, and proportions of the nose provide visual bases for the facial character of the person, which in turn facilitates facial recognition [36–39]. In forensic science, the estimation of external nose morphology is an important issue that could help identify people based on skulls. To this regard, the investigation of external nose morphology based on CBCT and 3dMD images in living subjects may provide further help to forensic anthropologists.

Numerous studies have explored the interrelationship between hard nasal bone and soft-tissue morphology of nose. Stephan et al. [10] examined four published methods used for predicting nose projection and pronasale position and

**Table 4** Means and standard deviations of the measurements for soft tissues (mm) in Chinese young adults

| Measurements | Total (n = 180) | | Male (n = 90) | | Female (n = 90) | | Sex difference |
| --- | --- | --- | --- | --- | --- | --- | --- |
| | Mean | SD | Mean | SD | Mean | SD | p value |
| Nasal bridge length | 48.75 | 3.61 | 50.68 | 2.92 | 46.86 | 3.21 | 0.000* |
| Nasal height | 55.41 | 3.92 | 57.58 | 3.23 | 53.29 | 3.34 | 0.000* |
| Nasal columella length | 17.02 | 1.86 | 17.81 | 1.93 | 16.24 | 1.43 | 0.000* |
| Alar width | 38.38 | 3.47 | 40.30 | 3.07 | 36.51 | 2.73 | 0.000* |
| Basis nasi angle | 78.75 | 7.02 | 78.21 | 7.52 | 79.27 | 6.50 | 0.315 |
| Alare angle | 42.10 | 4.28 | 43.27 | 3.08 | 40.95 | 4.95 | 0.000* |
| Nasal dorsum angle | 15.99 | 1.74 | 16.10 | 1.88 | 15.89 | 1.59 | 0.428 |
| Nasal tip angle | 106.41 | 9.21 | 106.09 | 11.83 | 106.72 | 5.63 | 0.649 |
| Nasolabial angle | 119.47 | 12.69 | 120.53 | 15.93 | 118.43 | 8.38 | 0.271 |
| Nasal tip protrusion | 23.67 | 3.99 | 24.46 | 4.63 | 22.90 | 3.10 | 0.009* |
| Basis nasi protrusion | 11.98 | 3.74 | 12.51 | 3.98 | 11.46 | 3.42 | 0.061 |

**Table 5** Correlation coefficients between hard- and soft-tissue measurements in males

|  | nasal width | nasal height | nasal bone length | alare angle | nasal dorsum angle | nasal tip angle | nasolabial angle | rhinion protrusion | nasospinale protrusion | nTr-rhiTr | rhiTr-alTr | alTr-nsTr | nTr-alTr | rhiTr-nsTr | nTr-nsTr |
|---|---|---|---|---|---|---|---|---|---|---|---|---|---|---|---|
| Nasal bridge length | 0.145 | 0.354* | 0.375* | −0.044 | 0.176 | −0.084 | 0.148 | 0.215 | −0.124 | 0.381 | −0.071 | 0.305* | 0.277* | 0.077 | 0.399* |
| Nasal height | 0.071 | 0.244 | 0.454* | −0.185 | −0.023 | 0.111 | −0.242 | −0.035 | −0.214 | 0.322 | 0.022 | 0.151 | 0.310 | 0.093 | 0.362* |
| Nasal columella length | −0.024 | 0.151 | 0.358* | −0.189 | 0.208 | −0.198 | −0.085 | 0.123 | −0.053 | 0.083 | 0.047 | −0.008 | 0.117 | 0.042 | 0.109 |
| Alar width | 0.241* | 0.009 | 0.06 | 0.177 | −0.236 | 0.201 | 0.205 | −0.185 | −0.039 | 0.134 | −0.021 | −0.109 | 0.101 | −0.072 | 0.049 |
| Basis nasi angle | 0.097 | −0.125 | −0.059 | 0.155 | −0.311* | 0.342* | 0.066 | −0.341* | 0.098 | 0.095 | −0.111 | −0.085 | −0.017 | −0.148 | −0.053 |
| Alare angle | 0.033 | −0.288 | −0.155 | 0.160 | −0.113 | 0.152 | 0.232 | −0.175 | 0.086 | −0.195 | 0.125 | −0.233* | −0.061 | 0.010 | −0.160 |
| Nasal dorsum angle | 0.094 | −0.009 | −0.082 | 0.058 | 0.188 | −0.228* | 0.068 | 0.156 | 0.143 | −0.206 | 0.133 | −0.056 | −0.062 | 0.102 | −0.084 |
| Nasal tip angle | −0.089 | −0.004 | −0.061 | −0.006 | −0.253 | 0.229 | −0.013 | −0.291* | −0.245* | 0.099 | −0.173 | 0.052 | −0.071 | −0.143 | −0.045 |
| Nasolabial angle | 0.052 | −0.029 | 0.073 | 0.029 | 0.031 | −0.062 | 0.005 | −0.074 | −0.198 | 0.043 | 0.150 | 0.073 | 0.177 | 0.180 | 0.201 |
| Nasal tip protrusion | 0.053 | 0.067 | 0.134 | −0.108 | −0.020 | −0.077 | 0.154 | 0.316* | 0.482* | −0.049 | 0.223 | −0.03 | 0.162 | 0.202 | 0.143 |
| Basis nasi protrusion | −0.048 | 0.002 | 0.025 | −0.116 | 0.021 | −0.062 | 0.189 | 0.355* | 0.499* | −0.123 | 0.145 | 0.058 | 0.023 | 0.168 | 0.048 |

**Table 6** Correlation coefficients between hard- and soft-tissue measurements in females

| | nasal width | nasal height | nasal bone length | alare angle | nasal dorsum angle | nasal tip angle | nasolabial angle | rhinion protrusion | nasospinale protrusion | nTr-rhiTr | rhiTr-alTr | alTr-nsTr | nTr-alTr | rhiTr-nsTr | nTr-nsTr |
|---|---|---|---|---|---|---|---|---|---|---|---|---|---|---|---|
| Nasal bridge length | 0.020 | 0.357* | 0.569* | −0.219 | 0.208 | −0.220 | −0.020 | 0.381* | 0.154 | 0.359* | 0.171 | 0.190 | 0.526* | 0.277* | 0.586* |
| Nasal height | 0.001 | 0.402* | 0.585* | −0.189 | 0.278* | −0.122 | −0.091 | 0.316* | 0.119 | 0.416* | 0.050 | 0.256* | 0.500* | 0.205 | 0.593* |
| Nasal columella length | 0.014 | 0.076 | 0.189 | 0.046 | 0.113 | −0.097 | 0.151 | 0.137 | 0.176 | 0.211 | 0.066 | 0.145 | 0.284* | 0.151 | 0.336* |
| Alar width | 0.278* | 0.098 | 0.085 | 0.247* | 0.077 | 0.137 | −0.103 | −0.037 | 0.022 | 0.121 | −0.089 | 0.036 | 0.070 | −0.061 | 0.083 |
| Basis nasi angle | 0.129 | −0.001 | −0.249* | 0.175 | −0.049 | 0.329* | −0.178 | −0.187 | −0.002 | −0.016 | −0.267* | −0.145 | −0.214 | −0.338* | −0.270 |
| Alare angle | 0.221 | −0.223 | −0.189 | 0.255* | −0.016 | 0.201 | 0.118 | −0.165 | 0.044 | −0.196 | 0.070 | −0.082 | −0.167 | 0.015 | −0.196 |
| Nasal dorsum angle | 0.015 | −0.092 | 0.007 | 0.081 | 0.038 | −0.111 | 0.132 | −0.003 | −0.016 | −0.018 | 0.112 | 0.022 | 0.062 | 0.118 | 0.069 |
| Nasal tip angle | −0.108 | −0.027 | −0.124 | 0.044 | −0.017 | 0.407* | −0.139 | −0.307 | −0.142 | −0.013 | −0.316* | 0.058 | −0.246 | −0.257* | 0.206 |
| Nasolabial angle | −0.067 | 0.071 | 0.144 | 0.015 | −0.166 | −0.064 | 0.305* | 0.082 | 0.049 | 0.117 | −0.031 | 0.144 | 0.108 | 0.060 | 0.169 |
| Nasal tip protrusion | −0.003 | 0.232 | 0.474* | −0.175 | −0.123 | −0.057 | 0.045 | 0.383* | 0.469* | 0.175 | 0.298* | 0.039 | 0.413* | 0.301* | 0.410* |
| Basis nasi protrusion | −0.041 | 0.104 | 0.365* | −0.172 | −0.206 | 0.142 | −0.019 | 0.257* | 0.460* | 0.093 | 0.206 | −0.023 | 0.254* | 0.177 | 0.230 |

**Table 7** Stepwise multiple regression equations for predicting soft nose according to hard nasal bone in males

| Measurement | Regression formula | SEE | $R^2$ | $p$ value |
|---|---|---|---|---|
| Nasal bridge length | 0.215*nasal bone length + 0.096*nasal height + 0.459*(alTr-nsTr) + 0.117*(nTr-nsTr) + 31.101 | 2.581 | 0.257 | 0.000 |
| Nasal height | 0.339*nasal height + 0.08*(nTr-nsTr) + 34.769 | 2.909 | 0.210 | 0.000 |
| Nasal columella length | 0.186* nasal height + 7.668 | 1.819 | 0.128 | 0.008 |
| Alar width | 0.324*nasal width + 32.485 | 3.001 | 0.158 | 0.024 |
| Basis nasi angle | − 0.094*nasal dorsum angle + 0.115*nasal tip angle − 0.696*rhinion protrusion + 72.817 | 6.943 | 0.178 | 0.001 |
| Alare angle | − 0.46*(alTr-nsTr) + 45.767 | 3.021 | 0.054 | 0.029 |
| Nasal dorsum angle | − 0.028*nasal tip angle + 19.936 | 1.712 | 0.038 | 0.009 |
| Nasal tip angle | −0.853*rhinion protrusion − 0.226*nasospinale protrusion + 117.678 | 8.876 | 0.083 | 0.001 |
| Nasolabial angle | − | − | − | − |
| Nasal tip protrusion | 0.273*rhinion protrusion + 0.446*nasospinale protrusion + 17.699 | 3.524 | 0.233 | 0.000 |
| Basis nasi protrusion | 0.16*rhinion protrusion + 0.473*nasospinale protrusion+7.141 | 3.295 | 0.232 | 0.000 |

suggested that two of the four traditional methods were inaccurate. Inada et al. [24] investigated the relationship between skeletal landmarks and nose morphology from cephalometric images in 80 preschool Japanese children and found that the soft-tissue nasal landmarks can be predicted from selected skeletal landmarks. Jennifer et al. [40] evaluated variations in nasal bone and aperture shape from 310 crania of black, white, and colored South Africans and compared the differences in the nasal aperture region between white and non-white South African groups. However, these had limitations in nasal approximation in that they only used two-dimensional methods or only utilized cadavers or skulls, and thus, the accuracy of measurement was questionable.

New radiological techniques, especially CBCT, allow the estimation of nose morphology in three dimensions. In 2015, Schlager et al. [41] analyzed the shape variance and symmetry of nasal from 267 Germans and 267 Chinese based on CT images. They explained the significant differences in nasal shape between the two populations and found that sex played a minor role in the observed shape variation. Recently, Lee et al. [13] and Ridel et al. [14] also used CBCT scans to investigate the relationship between the nasal bone and external nose morphology in the Korean and South African populations, which provided a new technology for predicting nasal morphology based on skeletal landmarks. However, they only analyzed the distances of the soft tissues of the nasal structure in the sagittal direction, whereas the detailed features of the external nose morphology in the frontal side were not illustrated. Thus, the present study analyzed the correlations between hard and soft tissues in the nasal region in three dimensions and tried to improve the accuracy of prediction for nose morphology reconstruction.

**Table 8** Stepwise multiple regression equations for predicting soft nose according to hard nasal bone in females

| Measurement | Regression formula | SEE | $R^2$ | $p$ value |
|---|---|---|---|---|
| Nasal bridge length | − 0.291*nasal bone length + 0.478*nasal height + 0.364*rhinion protrusion + 0.041*(nTr-rhiTr) − 0.071*(rhiTr-nsTr) + 0.311*(nTr-nsTr) + 10.550 | 2.510 | 0.314 | 0.000 |
| Nasal height | − 0.218*nasal bone length + 0.518*nasal height + 0.209*rhinion protrusion + 0.192*(nTr-rhiTr) − 0.159*(nTr-alTr) + 0.319*(nTr-nsTr) + 17.318 | 2.917 | 0.243 | 0.001 |
| Nasal columella length | − 0.033*(nTr-alTr) + 0.176*(nTr-nsTr) + 8.923 | 1.946 | 0.014 | 0.005 |
| Alar width | 0.334*nasal width + 0.078*alare angle + 26.539 | 2.657 | 0.079 | 0.027 |
| Basis nasi angle | − 0.296*nasal height + 0.340*nasal tip angle-0.207*(rhiTr-alTr) − 0.750*(rhiTr-nsTr) + 71.505 | 5.715 | 0.261 | 0.000 |
| Alare angle | 0.475*alare angle + 27.277 | 4.817 | 0.065 | 0.015 |
| Nasal dorsum angle | − | − | − | − |
| Nasal tip angle | 0.372*nasal tip angle − 0.862*(rhiTr-alTr) − 0.072*(rhiTr-nsTr) + 75.429 | 4.800 | 0.300 | 0.000 |
| Nasolabial angle | 0.303*nasolabial angle + 70.948 | 8.029 | 0.093 | 0.003 |
| Nasal tip protrusion | 0.309*nasal height + 0.027*rhinion protrusion + 0.358*nasospinale protrusion + 0.182*(rhiTr-alTr) + 0.037*(nTr-alTr) + 0.118*(nTr-nsTr) − 6.322 | 8.811 | 0.389 | 0.000 |
| Basis nasi protrusion | 0.432*nasal height − 0.270*rhinion protrusion + 0.593*nasospinale protrusion − 0.013*(nTr-alTr) − 10.388 | 2.923 | 0.303 | 0.000 |

**Table 9** Differences between measured value (MV) and predicted value (PV) in 30 males (test group)

|  | Mean of (MV-PV) | Mean of \|MV-PV\| | Maximum of \|MV-PV\| | Mininum of \|MV-PV\| | % 3 mm or 5° | ≤10% | t | p value of paired t test |
|---|---|---|---|---|---|---|---|---|
| Nasal bridge length | 0.57 ± 2.41 | 1.94 ± 1.50 | 6.25 | 0.09 | 25 (83.3%) | 29 (96.7%) | 1.311 | 0.200 |
| Nasal height | 0.46 ± 2.88 | 2.16 ± 1.92 | 9.01 | 0.08 | 23 (76.6%) | 29 (96.7%) | 0.880 | 0.386 |
| Nasal columella length | 0.07 ± 1.53 | 1.23 ± 0.88 | 3.00 | 0.01 | 30 (100%) | 30 (100%) | 0.270 | 0.789 |
| Alar width | −0.85 ± 3.69 | 3.02 ± 2.22 | 10.36 | 0.31 | 21 (70.0%) | 27 (90.0%) | −1.26 | 0.219 |
| Basis nasi angle | 0.75 ± 6.35 | 5.17 ± 3.65 | 13.02 | 0.34 | 17 (56.7%) | 25 (83.3%) | 0.654 | 0.518 |
| Alare angle | −1.07 ± 2.98 | 2.47 ± 1.94 | 7.62 | 0.16 | 26 (86.7%) | 28 (93.3%) | −1.97 | 0.059 |
| Nasal dorsum angle | −0.18 ± 1.45 | 1.29 ± 0.64 | 2.58 | 0.22 | 30 (100%) | 30 (100%) | −0.69 | 0.493 |
| Nasal tip angle | 1.47 ± 5.80 | 4.64 ± 3.69 | 12.89 | 0.00 | 20 (66.7%) | 27 (90.0%) | 1.396 | 0.173 |
| Nasolabial angle | – | – | – | – | – | – | – | – |
| Nasal tip protrusion | 0.99 ± 3.27 | 2.91 ± 1.72 | 6.42 | 0.04 | 28 (93.3%) | 28 (93.3%) | 1.672 | 0.105 |
| Basis nasi protrusion | 0.98 ± 3.86 | 3.14 ± 2.39 | 8.15 | 0.05 | 25 (83.3%) | 26 (86.7%) | 1.398 | 0.173 |

To assess the accuracy of this novel method for nose reconstruction, we used a test group to validate the method in Chinese young adults. To eliminate the influence of low resolution of CBCT and further improve the accuracy in soft tissue measurement, we used facial images captured by a 3dMD photogrammetry system to replace soft-tissue images from CBCT. In our study, we selected representative craniometric landmarks [nasion (n), rhinion (rhi), nasospinale (ns), alare (al), and prosthion (pro)] and capulometric landmarks [soft Nasion (N), Pronasale (Prn), Subnasale (Sn), Ala (Al), and Labial superius (Ls)] in the mid-facial region, validating whether the three-dimensional linear distances and angulations among these can accurately depict nasal region. Three-dimensional images scanned by CBCT and 3dMD were superimposed to evaluate hard and soft tissue simultaneously. The 3D images can be rotated and viewed from different angles to help identify anatomical landmarks precisely. The utilization of 3D coordinate values allowed us to automatically obtain measurements.

Therefore, the superimposed images were considered the ideal method for measurement of hard nasal bone and corresponding soft tissue.

Meng et al. [42] found that complete development of nose height, depth, and inclination in females is achieved by age 16, whereas for males, it could continue to develop until 18 or later. Therefore, we selected subjects with ages between 20 and 30 years to eliminate developmental factors caused by age in nasal region measurements. For measurements of the hard nasal, we obtained higher values in most measurements (nasal width, nasal height, nasal bone length, rhinion protrusion, nTr-rhiTr, rhiTr-alTr, nTr-alTr, rhiTr-nsTr, and nTr-nsTr) in males compared to females. Nevertheless, males showed smaller alare angles and nasal tip angles, which suggested that females shared more stereoscopic nasal structures. For the soft-tissue morphology of the nose, the results were similar to that of hard nasal bones. Compared to females, it showed greater distances in Nasal bridge length, Nasal height, Nasal

**Table 10** Differences between measured value (MV) and predicted value (PV) in 30 females (test group)

|  | Mean of (MV-PV) | Mean of \|MV-PV\| | Max of \|MV-PV\| | Min of \|MV-PV\| | % 3 mm or 5° | ≤10% | t | p value of paired t test |
|---|---|---|---|---|---|---|---|---|
| Nasal bridge length | 1.23 ± 2.77 | 2.51 ± 1.65 | 5.99 | 0.07 | 21 (70.0%) | 26 (86.7%) | 2.442 | 0.210 |
| Nasal height | 0.35 ± 2.70 | 2.10 ± 1.70 | 7.22 | 0.14 | 22 (73.3%) | 25 (83.3%) | 0.732 | 0.470 |
| Nasal columella length | −0.13 ± 1.50 | 1.15 ± 0.94 | 3.62 | 0.02 | 28 (93.3%) | 28 (93.3%) | −0.49 | 0.629 |
| Alar width | 0.16 ± 2.74 | 2.32 ± 1.40 | 5.10 | 0.10 | 23 (76.7%) | 25 (83.3%) | 0.321 | 0.750 |
| Basis nasi angle | 0.70 ± 6.00 | 5.09 ± 3.10 | 11.42 | 0.11 | 18 (60.0%) | 22 (73.3%) | 0.648 | 0.522 |
| Alare angle | 0.93 ± 3.15 | 2.48 ± 2.10 | 7.94 | 0.09 | 27 (90.0%) | 30 (100%) | 1.625 | 0.115 |
| Nasal dorsum angle | – | – | – | – | – | – | – | – |
| Nasal tip angle | 0.48 ± 4.32 | 3.49 ± 2.51 | 9.28 | 0.02 | 21 (70.0%) | 29 (96.7%) | 0.617 | 0.542 |
| Nasolabial angle | 0.02 ± 11.06 | 8.38 ± 7.05 | 23.29 | 0.26 | 15 (50.0%) | 21 (70.0%) | 0.014 | 0.989 |
| Nasal tip protrusion | −0.43 ± 2.61 | 1.99 ± 1.70 | 6.15 | 0.03 | 25 (83.3%) | 28 (93.3%) | −0.91 | 0.370 |
| Basis nasi protrusion | 0.32 ± 2.97 | 2.43 ± 1.68 | 5.87 | 0.07 | 23 (76.7%) | 27 (90.0%) | 0.600 | 0.553 |

columella length, Alar width, and Nasal tip protrusion, as well as larger angulations in Alare angle in males. Overall, males showed larger structures in the mid-facial region compared to females. Considering the variance between sexes, the morphology and size of the nasal region may be potentially used for sex discrimination.

Several measurements of the hard nasal showed a significant correlation with the related soft nose in both sexes. For example, the nasal bone length showed statistically significant correlations with Nasal bridge length (males 0.375, females 0.569) and Nasal height (males 0.454, females 0.585). Besides, nasospinale protrusion also showed significant correlations with Nasal tip protrusion (males 0.482, females 0.499) and Basis nasi protrusion (males 0.469, females 0.460). However, the alare angle, nasolabial angle, nTr-rhiTr, rhiTr-alTr, and rhiTr-nsTr did not show any correlations with the external nose morphology in males. However, in females, these measurements showed different situations, some of which were not so strong. Compared with previous studies conducted by Lee [13] and Ridel [14], the correlation coefficients between hard nasal bone and related soft tissues in our study were relatively lower. One possible reason might be that they only analyzed the correlations between skeletal and soft tissues of the nasal structures in the sagittal dimension, while we explored the relationships between skeletal and soft tissue of nasal structure in three dimensions. It seems that our estimation method was difficult but more accurate.

Overall, our study indicated that nasal bone structures can play an important role in estimating nose morphology. All of the formulas established for predicting nose morphology showed significant correlations except Nasolabial angle in males and Nasal dorsum angle in females, which suggested that angulations of the nose are apparently more difficult to predict than linear distances. Although the coefficients of determination in some stepwise multiple regression equations were low (males 0.038 of Nasal dorsum angle, females 0.014 of Nasal columella length), no significant differences were observed between the measured values and predicted values in the test group. Moreover, the accuracy for predicting nose morphology in the test group was relatively high. The proportion of subjects with measurement errors < 10% was > 86.7% in males and 70.0% in females, which indicated that the methods for nose reconstruction developed in this study were useful and reliable.

Currently, many studies have investigated nose morphology to reconstruct nasal region of mid-face. However, there were no related studies exploring the relationships between hard nasal bone and soft tissues of the nose in three dimensions in the Chinese population. Besides, in our study, we first superimposed CBCT and 3dMD images to improve the accuracy for nose morphology reconstruction. We hope that our novel method could be applied to forensic practice and tested by other populations.

## Conclusions

The superimposition of CBCT and 3dMD images is a reliable method in nasal morphology reconstruction. The results of this study provided different formulas for predicting nose morphology based on the nasal bone structures in young Chinese subjects. The pronasale, subnasale, and alare positions can be potentially used as predictors for the reconstruction of the nose. Our further research should focus on increasing the sample size to establish a more powerful facial database for the Chinese population. Meanwhile, other factors such as age, skeletal facial type, and facial proportion should also be taken into consideration.

## Compliance with ethical standards

Ethical approval was granted by the ethics committee of Stomatological Hospital of Xi'an Jiaotong University.

**Conflict of interest** The authors declare that they have no conflict of interest.

**Ethical approval** All procedures performed in studies involving human participants were in accordance with the ethical standards of the institutional and/or national research committee and with the 1964 Helsinki declaration and its later amendments or comparable ethical standards. For this type of study, formal consent is not required.

**Informed consent** Informed consent was provided by all individual participants included in the study, according to the Declaration of Helsinki.

## References

1. Utsuno H, Kageyama T, Uchida K, Kibayashi K, Sakurada K, Uemura K (2016) Pilot study to establish a nasal tip prediction method from unknown human skeletal remains for facial reconstruction and skull photo superimposition as applied to a Japanese male populations. J Forensic Legal Med 38:75–80
2. Sarilita E, Rynn C, Mossey PA, Black S, Oscandar F (2018) Nose profile morphology and accuracy study of nose profile estimation method in Scottish subadult and Indonesian adult populations. Int J Legal Med 132(3):923–931
3. Melo PM, Ribeiro DLR, Santos RLD, De Santana C-L, Cruz JPP (2014) Soft tissue thickness in young north eastern Brazilian individuals with different skeletal classes. J Forensic Legal Med 22(1): 115–120
4. Codinha S (2009) Facial soft tissue thicknesses for the Portuguese adult population. Forensic Sci Int 184(1–3):80 e1–7
5. Garlie TN, Saunders SR (1999) Midline facial tissue thicknesses of subadults from a longitudinal radiographic study. J Forensic Sci 44(1):61
6. Johari M, Esmaeili F, Hamidi H (2017) Facial soft tissue thickness of midline in an Iranian sample: MRI study. Open Dentistry J 11(Suppl-1, M6):375–383

7. Strapasson RAP, Herrera LM, Melani RFH (2017) Forensic facial reconstruction: relationship between the alar cartilage and piriform aperture. J Forensic Sci 62(6):1460–1465

8. Rynn C, Wilkinson CM, Peters HL (2010) Prediction of nasal morphology from the skull. Forensic Sci Med Pathol 6(1):20–34

9. Hoffman BE, McConathy DA, Coward M, Saddler L (1991) Relationship between the piriform aperture and interalar nasal widths in adult males. J Forensic Sci 36(4):1152–1161

10. Rynn C, Wilkinson CM (2006) Appraisal of traditional and recently proposed relationships between the hard and soft dimensions of the nose in profile. Am J Phys Anthropol 130(3):364–373

11. Kobyliansky E, Balueva T, Veselovskaya E, Arensburg B (2008) Facial image of Biblical Jews from Israel. Anthropol Anz 66(2): 167–190

12. Stephan CN (2003) Anthropological facial reconstruction—recognizing the fallacies, 'unembracing' the errors, and realizing method limits. Sci Justice 43(4):193–200

13. Lee KM, Lee WJ, Cho JH, Hwang HS (2014) Three-dimensional prediction of the nose for facial reconstruction using cone-beam computed tomography. Forensic Sci Int 236:194 e1–5

14. Ridel AF, Demeter F, Liebenberg J, L'Abbe EN, Vandermeulen D, Oettle AC (2018) Skeletal dimensions as predictors for the shape of the nose in a South African sample: a cone-beam computed tomography (CBCT) study. Forensic Sci Int 289:18–26

15. Stephan CN, Davidson PL (2008) The placement of the human eyeball and canthi in craniofacial identification. J Forensic Sci 53(3):612–619

16. Stephan CN, Huang AJ, Davidson PL (2009) Further evidence on the anatomical placement of the human eyeball for facial approximation and craniofacial superimposition. J Forensic Sci 54(2):267–269

17. Clarys JP, Provyn S, Marfell-Jones MJ (2005) Cadaver studies and their impact on the understanding of human adiposity. Ergonomics 48(11–14):1445–1461

18. Domaracki M, Stephan CN (2006) Facial soft tissue thicknesses in Australian adult cadavers. J Forensic Sci 51(1):5–10

19. Tedeschi-Oliveira SV, Melani RF, de Almeida NH, de Paiva LA (2009) Facial soft tissue thickness of Brazilian adults. Forensic Sci Int 193(1–3):127 e1–7

20. El-Mehallawi IH, Soliman EM (2001) Ultrasonic assessment of facial soft tissue thicknesses in adult Egyptians. Forensic Sci Int 117(1–2):99–107

21. De Greef S, Claes P, Vandermeulen D, Mollemans W, Suetens P, Willems G (2006) Large-scale in-vivo Caucasian facial soft tissue thickness database for craniofacial reconstruction. Forensic Sci Int 159(Suppl 1):S126–S146

22. Wilkinson CM (2002) In vivo facial tissue depth measurements for white British children. J Forensic Sci 47(3):459–465

23. Stephan CN, Henneberg M, Sampson W (2003) Predicting nose projection and pronasale position in facial approximation: a test of published methods and proposal of new guidelines. Am J Phys Anthropol 122(3):240–250

24. Inada E, Saitoh I, Hayasaki H, Iwase Y, Kubota N, Tokemoto Y, Yamada C, Yamasaki Y (2009) Relationship of nasal and skeletal landmarks in lateral cephalograms of preschool children. Forensic Sci Int 191(1–3):111 e1–4

25. Davy-Jow SL, Decker SJ, Ford JM (2012) A simple method of nose tip shape validation for facial approximation. Forensic Sci Int 214(1–3):208 e1–3

26. Maltais LG, Lynnerup N, Hoppa RD (2016) Validation of the new interpretation of Gerasimov's nasal projection method for forensic facial approximation using CT data(.). J Forensic Sci 61(Suppl 1): S193–S200

27. Chen F, Chen Y, Yu Y, Qiang Y, Liu M, Fulton D, Chen T (2011) Age and sex related measurement of craniofacial soft tissue thickness and nasal profile in the Chinese population. Forensic Sci Int 212(1–3):272 e1–6

28. Lambros VS (2013) Discussion: soft-tissue mobility of the lower face depending on positional changes and age: a three-dimensional morphometric surface analysis. Plast Reconstr Surg 131(2):382–383

29. Marin F, Mansour KB, Demeter F, Frey P (2015) Displacement of facial soft tissues in upright versus supine positions. Comput Methods Biomech Biomed Eng 18(sup1):1988–1989

30. Weinberg SM, Naidoo S, Govier DP, Martin RA, Kane AA, Marazita ML (2006) Anthropometric precision and accuracy of digital three-dimensional photogrammetry: comparing the Genex and 3dMD imaging systems with one another and with direct anthropometry. J Craniofac Surg 17(3):477–483

31. Aldridge K, Boyadjiev SA, Capone GT, DeLeon VB, Richtsmeier JT (2005) Precision and error of three-dimensional phenotypic measures acquired from 3dMD photogrammetric images. Am J Med Genet A 138A(3):247–253

32. Hwang HS, Lee KM, Uhm GS, Cho JH, McNamara JA Jr (2013) Use of reference ear plug to improve accuracy of lateral cephalograms generated from cone-beam computed tomography scans. Korean J Orthod 43(2):54–61

33. Duran GS, Dindaroglu F, Gorgulu S (2017) Three-dimensional evaluation of social smile symmetry. Angle Orthod 87(1):96–103

34. Maal TJ, Verhamme LM, van Loon B, Plooij JM, Rangel FA, Kho A, Bronkhorst EM, Berge SJ (2011) Variation of the face in rest using 3D stereophotogrammetry. Int J Oral Maxillofac Surg 40(11): 1252–1257

35. Statistical Methods for Medical and Biological Students. The Indian Medical Gazette, 1940. 75(10): p. 638–638

36. Hefner JT (2009) Cranial nonmetric variation and estimating ancestry*. J Forensic Sci 54(5):985–995

37. Farkas LG, Kolar JC, Munro IR (1986) Geography of the nose: a morphometric study. Aesthet Plast Surg 10(4):191–223

38. Wang D, Qian G, Zhang M, Farkas LG (1997) Differences in horizontal, neoclassical facial canons in Chinese (Han) and North American Caucasian populations. Aesthet Plast Surg 21(4):265–269

39. Fernandez-Riveiro P, Smyth-Chamosa E, Suarez-Quintanilla D, Suarez-Cunqueiro M (2003) Angular photogrammetric analysis of the soft tissue facial profile. Eur J Orthod 25(4):393–399

40. McDowell JL, Kenyhercz MW, L'Abbe EN (2015) An evaluation of nasal bone and aperture shape among three South African populations. Forensic Sci Int 252:189 e1–7

41. Schlager S, Rudell A (2015) Analysis of the human osseous nasal shape—population differences and sexual dimorphism. Am J Phys Anthropol 157(4):571–581

42. Meng HP, Goorhuis J, Kapila S, Nanda RS (1988) Growth changes in the nasal profile from 7 to 18 years of age. Am J Orthod Dentofac Orthop 94(4):317–326